

# Novel visual illusions related to Vasarely's 'nested squares' show that corner salience varies with corner angle

Xoana G Troncoso<sup>§</sup>, Stephen L Macknik, Susana Martinez-Conde<sup>¶</sup>

Department of Neurobiology, Barrow Neurological Institute, 350 W Thomas Road, Phoenix, AZ 85013, USA; e-mail: [smart@neuralcorrelate.com](mailto:smart@neuralcorrelate.com); <sup>§</sup> also Gatsby Computational Neuroscience Unit, University College London, 17 Queen Square, London WC1N 3AR, UK

Received 14 November 2004, in revised form 23 January 2005

**Abstract.** Vasarely's 'nested-squares' illusion shows that 90° corners can be more salient perceptually than straight edges. On the basis of this illusion we have developed a novel visual illusion, the 'Alternating Brightness Star', which shows that sharp corners are more salient than shallow corners (an effect we call 'corner angle salience variation') and that the same corner can be perceived as either bright or dark depending on the polarity of the angle (ie whether concave or convex: 'corner angle brightness reversal'). Here we quantify the perception of corner angle salience variation and corner angle brightness reversal effects in twelve naive human subjects, in a two-alternative forced-choice brightness discrimination task. The results show that sharp corners generate stronger percepts than shallow corners, and that corner gradients appear bright or dark depending on whether the corner is concave or convex. Basic computational models of center-surround receptive fields predict the results to some degree, but not fully.

## 1 Introduction

Vasarely's 'nested-squares' illusion (Vasarely 1970) shows that, in a luminance gradient composed of concentric squares, 90° corners generate illusory 'folds', which appear more salient (ie either brighter or darker) than the adjacent flat (non-corner) regions of each individual square (figure 1). This classic illusion has been described often (Hurvich 1981; Kaiser 1996; Morgan 1996; Adelson 1999; McArthur and Moulden 1999). However, the strength of the effect has never been quantified or tested systematically by computational, psychophysical, or neurophysiological techniques. Here we quantify the strength of Vasarely's nested-squares illusion, and other related effects, with psychophysical techniques (in a two-alternative forced-choice brightness discrimination task) and also with basic computational models of early visual function. The results offer insights into the possible neural mechanisms responsible for these effects, and may help to explain corner perception in general.

### 1.1 *The Alternating Brightness Star illusion*

In Vasarely's artworks, each gradient fold is constructed from a series of nested squares. That is, the corner angle is exactly 90°. In order to test the strength of the illusory folds generated by Vasarely's corner gradients, we started by varying the angles of the corners. In doing this, we discovered a novel visual illusion, which we called the Alternating Brightness Star (Martinez-Conde and Macknik 2001). Figure 2 shows several Alternating Brightness Stars, made of concentric stars arranged in gradients of increasing or decreasing luminance. Bright or dark illusory folds can be perceived, depending on the polarity of the corner angle (whether the angles of the corners are concave or convex). We called this effect 'corner angle brightness reversal' (CABR). An irregular version of the Alternating Brightness Star illusion (figures 2c and 2f) furthermore shows that the strength of the illusion depends on how shallow or sharp the angle is. We called this effect 'corner angle salience variation' (CASV): for shallow corner angles (figure 2c, angle  $\beta$ ) the effect is weak, whereas for sharp corner

<sup>¶</sup> Author to whom all correspondence should be addressed.

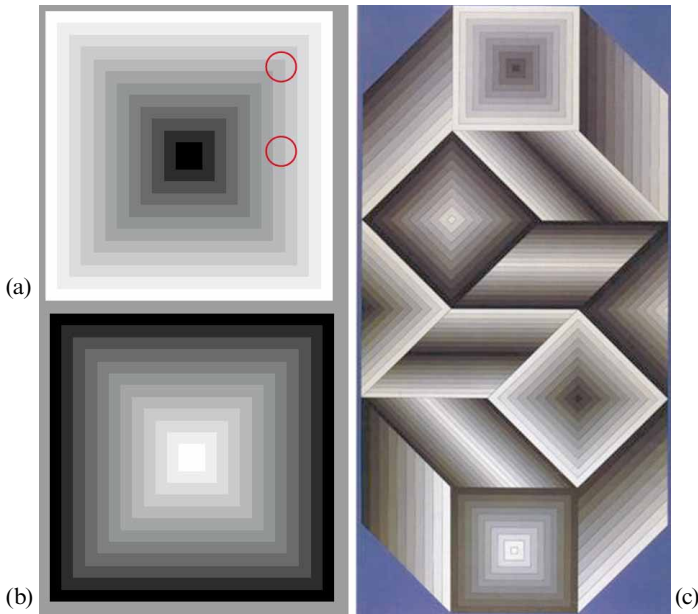


**Figure 1.** Vasarely's nested-squares illusion. (a) Nested-squares illusion based on Vasarely's *Arcturus* (Vasarely 1970). The stimulus is made out of multiple concentric squares of increasing luminance (going from black in the center to white at the outermost edge). The stimulus is reminiscent of a Chevreul staircase (Chevreul 1839) in which the linear luminance steps are formed by concentric squares rather than by parallel bands. The physical luminance of each individual square remains constant at all points, but the corners of the squares appear perceptually darker than the straight edges, forming an X-shape that seems to radiate from the very center of the figure. The two red circles indicate two regions that appear to have significantly different brightness. The area inside the upper red circle has higher average luminance than the region inside the lower circle; however, the region inside the upper circle appears perceptually darker. (b) Nested-squares stimulus, with a gradient of decreasing luminance (from the center to the outside). (c) Vasarely's *Utem* (1981). Reproduced, with permission of the Vasarely Foundation, from Vasarely (1982). Note the four sets of nested squares. The two nested squares of decreasing luminance (from the center to the outside) have bright illusory diagonals. The two nested squares of increasing luminance (from the center to the outside) have dark illusory diagonals.

angles (figure 2c, angle  $\alpha$ ) the illusory effect is strong. The CASV effect cannot be observed with regular polygonal constructs (as in figures 2a, 2b, 2d, and 2e) because regular polygons by definition have non-varying corner angles. These effects may be related to a previous anecdotal observation by von Békésy, in which he briefly and qualitatively described the varying extents of apparent saturation in individual yellow gelatin wedges cut at different angles (von Békésy 1968).

## 2 Methods

### 2.1 Subjects

All subjects were naive adult volunteers (nine females, three males), with normal or corrected-to-normal vision. Each subject participated in 10 experimental sessions, of  $\sim 1$  h each, and was paid \$15 per session. Experiments were carried out under the guidelines of the Barrow Neurological Institute's Institutional Review Board (protocol number 04BN039).

### 2.2 Experimental design

Subjects rested their head on a chin-rest, 57 cm from a linearized video monitor (Barco Reference Calibrator V). Subjects were asked to fixate a small cross ( $1 \text{ deg} \times 1 \text{ deg}$ ) within a  $3.5 \text{ deg}$  fixation window while visual stimuli were presented (figure 3). To ensure proper fixation, eye position was measured non-invasively with a video-based eye-movement monitor (EyeLink II, SR Research).

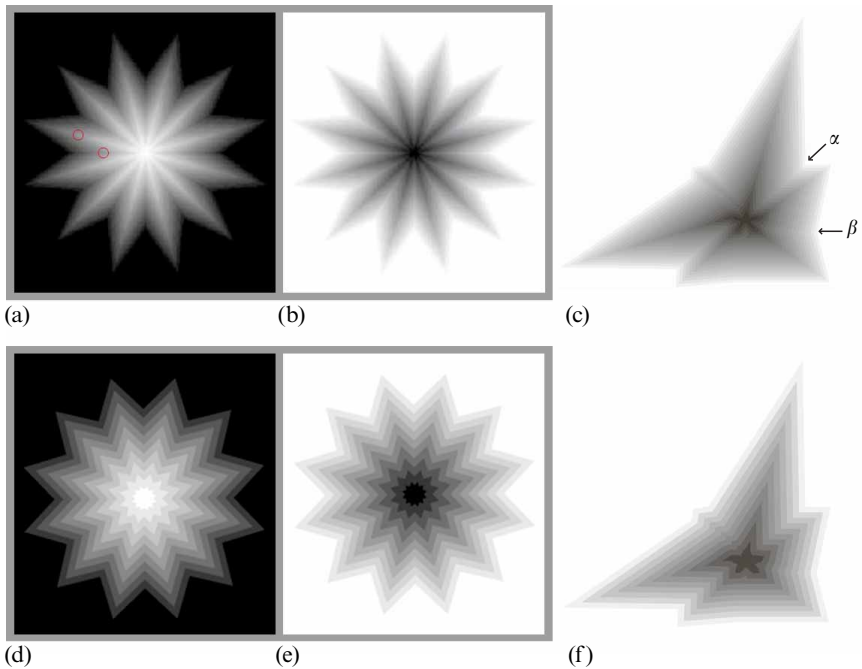


**Figure 2.** The Alternating Brightness Star illusion (Martinez-Conde and Macknik 2001). (a) and (b) Regular versions. The stimulus is made of concentric stars of graded luminance. In (a), the innermost star is white; the outermost star is black; in (b), the innermost star is black; the outermost star is white. The gradient from the center to the outside has 100 luminance steps. The illusory corner-folds that radiate from the center appear as light or dark depending on the polarity of the corner angle [corner angle brightness reversal (CABR) effect], and on the direction of the luminance gradient. However, all illusory folds are physically equal to each other in luminance. The two red circles in (a) indicate physically equivalent points in the luminance gradient. (c) An irregular version of the Alternating Brightness Star illusion illustrates the corner angle salience variation (CASV) effect. The illusory folds appear more salient with sharp corners (as in angle  $\alpha$ ), and less salient with shallow corners (as in angle  $\beta$ ). Here the folds also appear perceptually light or dark depending on the polarity of the corner angle (concave or convex). (d), (e), and (f) 10-luminance-step versions of the Alternating Brightness Stars shown in (a), (b), and (c), respectively. The individual stars forming the polygonal constructs are easy to identify.

To test the magnitude of the illusory percept, we conducted a two-alternative forced-choice brightness discrimination between illusory corner gradients (comparator stimuli) and non-illusory flat gradients (standard stimuli). At the beginning of each trial, a red fixation cross (on a grey background) was displayed on the monitor. Once the subject fixated the cross, two sets of stimuli appeared simultaneously: the standard and the comparator (one to the right and one to the left of the fixation cross—see figure 3). The size of the standard was 18 deg (h)  $\times$  0.5 deg (w), and that of the comparator was 18 deg (h)  $\times$  4 deg (w). Both comparator and standard stimuli were centered at 3° of eccentricity.

The comparator was a corner-gradient fold of 100 luminance steps with one of 13 possible angles:  $\pm 15^\circ$ ,  $\pm 30^\circ$  (figure 3b),  $\pm 45^\circ$ ,  $\pm 75^\circ$  (figure 3c),  $\pm 105^\circ$ ,  $\pm 135^\circ$  (for both illusory dark and bright folds), and  $180^\circ$ , which is a flat gradient (figure 3d). To construct the standard stimulus, we first drew five non-illusory  $180^\circ$  gradients of 100 steps each. We then divided each gradient into 11 luminance segments, which we pseudorandomly scrambled. Finally, we stacked all luminance segments into a long vertical stripe. Thus the entire standard stripe contained 55 segments total. Red bars were displayed to the sides of the standard and comparator stimuli, to indicate

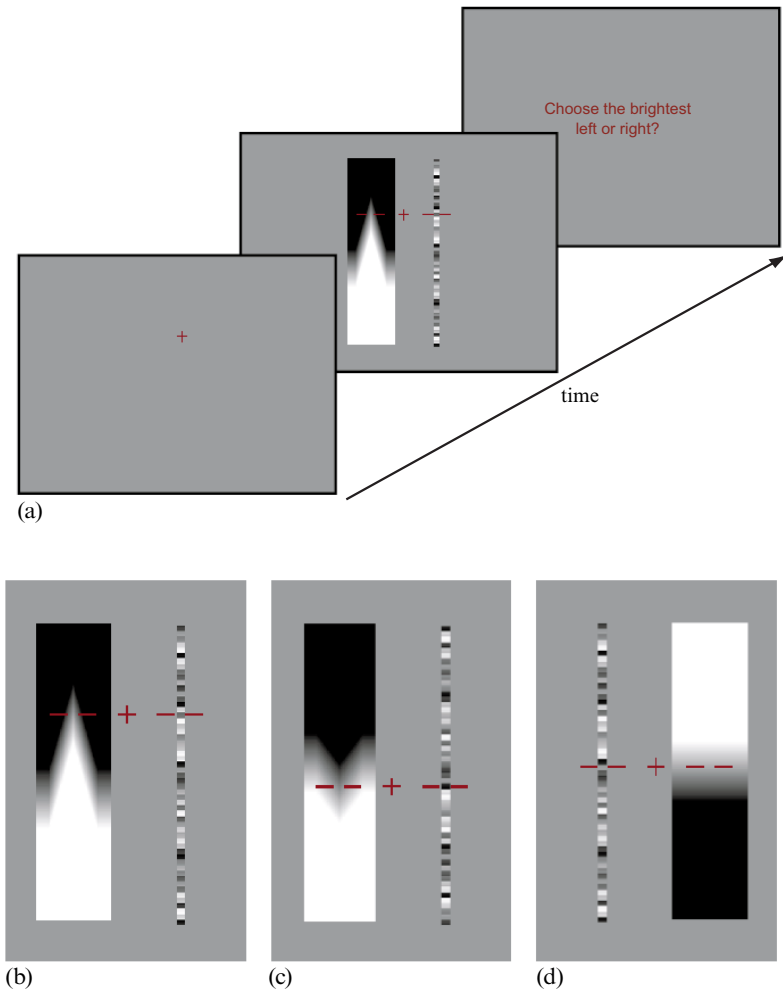


**Figure 3.** Psychophysical design. (a) Monitor display during time course of a single trial. (b), (c), and (d) Three different stimulus presentations of the brightness discrimination task (out of 572 possible conditions, see section 2 for details).

precisely the parts of the stimuli to be compared. These red bars were always drawn at the same height as the point of 50% luminance of the corner gradient in the comparator. Thus the vertical position of the red bars on the monitor varied as a function of the angle of the corner gradient. The fixation point and red bars on the standard were drawn at the same vertical position as the red bars over the comparator. The standard stripe was drawn so that there was an equal chance of any one of the 11 possible luminance segments to be selected by the horizontal red bars. We made sure that the red bars were always in the center of one of the segments. After 2 s, all stimuli disappeared.

The subject's task was to compare the brightness of the pixel positioned precisely in the center between the inner ends of the red bars on the standard stimulus, to the brightness of the same point on the comparator stimulus. The point of 50% luminance in the corner gradient of the comparator was compared against all possible luminances of the standard, for all corner angles tested. Since the discrimination point on the comparator was always of 50% luminance, the physical difference between the comparator and the standard was a function of the luminance of the segment within

the standard stimulus indicated by the red bars. Thus, if a 50% luminance standard segment appeared perceptually different from the comparator, and this varied as a function of corner angle of the comparator stimulus, then the difference was not physical and it must have been caused by the illusory effects of corner angle. Half of the subjects ( $n = 7$ ) indicated, by pressing the left/right keys on a keyboard, which stimulus appeared *brighter* at the discrimination point (the comparator or the standard). To control for potential bias due to the choosing of a brighter stimulus, the other half of the subjects ( $n = 5$ ) indicated which stimulus appeared darker. These two groups were later averaged to control for criterion effects. The design was further controlled for effects of criterion, by giving subjects a bright-appearing comparator in half the trials, and a dark-appearing comparator in the other half of the trials. The experiment was counterbalanced for potential left/right and up/down criterion effects by ensuring that the comparator was presented half the time on the left, and half the time on the right, with the bright half of the gradient on the upper half of the comparator half the time. Subjects did not have to wait until the stimuli turned off to indicate their decision, and could answer as soon as they were ready, in which case the stimuli were removed from the screen and the trial ended at the time of the subject's key-press. Standard and comparator had the same average luminance (50% gray) in all conditions. If the subject broke fixation (as measured by EyeLink II), the trial was aborted, and replaced in the pseudorandom trial stream to be re-run later.

The summary of all conditions ( $n = 572$ ) was as follows:

- 2 screen positions: left and right
- 2 gradient directions: bright on top, dark on top
- 13 corner angles:  $\pm 15^\circ$ ,  $\pm 30^\circ$ ,  $\pm 45^\circ$ ,  $\pm 75^\circ$ ,  $\pm 105^\circ$ , and  $\pm 135^\circ$ , plus  $180^\circ$  (flat gradient)
- 11 standard luminances: 5%, 14%, 23%, 32%, 41%, 50%, 59%, 68%, 77%, 86%, and 95%

For each subject, each combination of gradient direction (ie bright on top versus dark on top) and corner angle was presented 20 times, over 10 sessions (2 trials per session per combination).

Psychometric curves were obtained fitting the data with logistic functions by a maximum-likelihood procedure (Wichmann and Hill 2001).

### 2.3 Center – surround simulations

We modeled center – surround receptive fields as difference-of-Gaussians (DOG) filters (Rodieck 1965; Enroth-Cugell and Robson 1966):

$$\begin{aligned} \text{Receptive-field}(x, y) &= \text{Center}(x, y) - \text{Surround}(x, y) \\ &= k_c \exp[-(x/r_c)^2 - (y/r_c)^2] - k_s \exp[-(x/r_s)^2 - (y/r_s)^2], \end{aligned}$$

where  $r_c$  and  $r_s$ , or the 'radius' of center and surround, represent the distance over which the sensitivities of center and surround fall to  $1/e$  of the peak value;  $k_c$  and  $k_s$  represent the relative strengths of center and surround.

## 3 Results

### 3.1 Qualitative observations on the CABR effect

As predicted by the CABR effect described earlier, the perceived sign of the illusory fold depended on the interaction between the polarity of the angle (concave, or upwards versus convex, or downwards) and the direction of the gradient (black-to-white versus white-to-black). Black-to-white gradients (top-to-bottom) led to bright illusory folds when presented with upwards angles (as in figure 3b), whereas the same gradient direction led to dark illusory folds when presented with downwards angles (as in figure 3c). Conversely, white-to-black gradients (top-to-bottom) led to bright illusory folds when presented with downwards angles, and to dark illusory folds when presented with upwards angles.

The summary of the qualitative perceptual effects with top-to-bottom gradients was as follows:

- (1) black-to-white gradient + upwards angle = bright percept;
- (2) white-to-black gradient + downwards angle = bright percept;
- (3) black-to-white gradient + downwards angle = dark percept;
- (4) white-to-black gradient + upwards angle = dark percept.

### 3.2 Psychophysical test

We calculated the point of subjective equality (PSE) for each comparator (ie its matching luminance in the non-illusory standard) by determining the point on the psychometric curve (figure 4a) in which the comparator appeared more salient than the standard in 50% of the trials [averaged over all subjects, and collapsed across conditions (1), (2), (3), and (4) described above]. The illusory enhancement for each corner angle was calculated as the difference between the PSE for a  $180^\circ$  non-illusory gradient and the

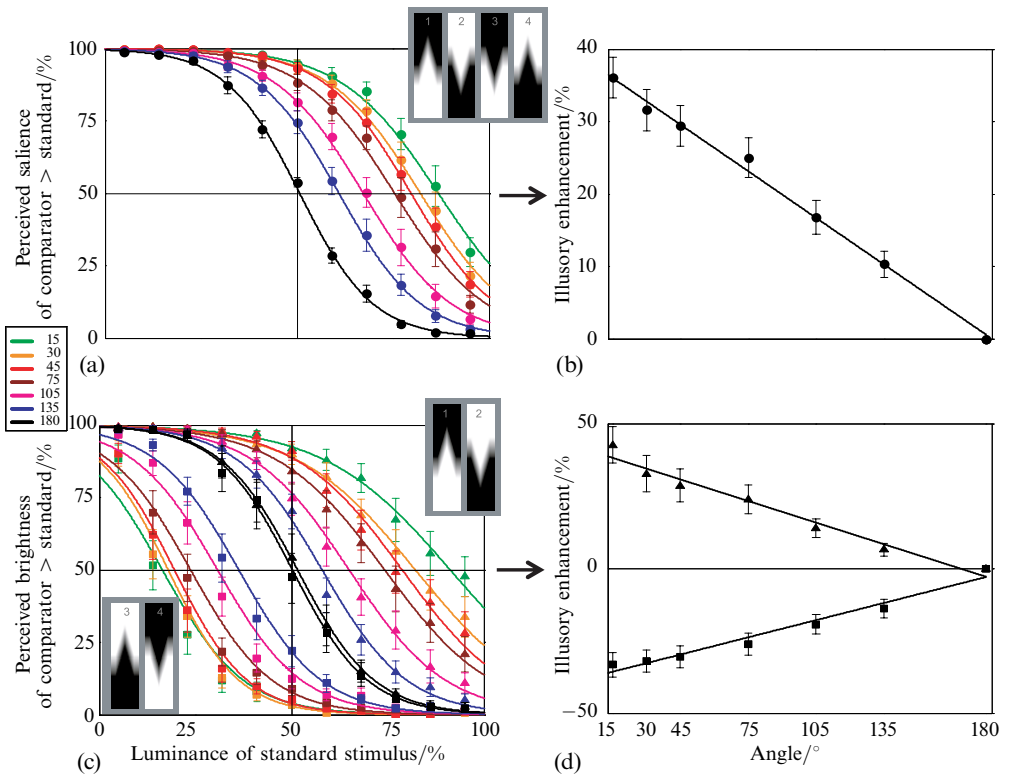


**Figure 4.** Psychophysical results. (a) Psychometric functions for the different corner angles are plotted in different colors. Gradient and angle polarities are collapsed: ie we have averaged together the conditions where the illusory folds of the comparator looked dark (inverted  $x$ -axis from figure 4c) and the conditions where they looked bright (non-inverted  $x$ -axis from figure 4c). The inset shows illustrations of the 4 collapsed conditions, for a  $30^\circ$  angle. (b) Illusory enhancement of the PSEs with respect to the control condition ( $180^\circ$  gradient) for the different comparator corner angles. The illusory enhancement decreases linearly as the angle of the comparator corner gradient becomes shallower (CASV effect). (c) Same data as in (a), but the conditions in which the illusory fold looked bright (triangles), and the conditions in which the illusory fold looked dark (squares) are presented separately (see insets). The PSEs for conditions 1 and 2 (see insets) fall above the point of 50% luminance in the standard stimulus. The PSEs for conditions 3 and 4 (see inset) fall below the point of 50% luminance in the standard stimulus (CABR effect). (d) Illusory enhancement of brightness (triangles) and darkness (squares) perception, as a function of corner angle. Error bars in (a), (b), (c), and (d) represent the  $\pm 1$  SEM for all subjects in each condition.

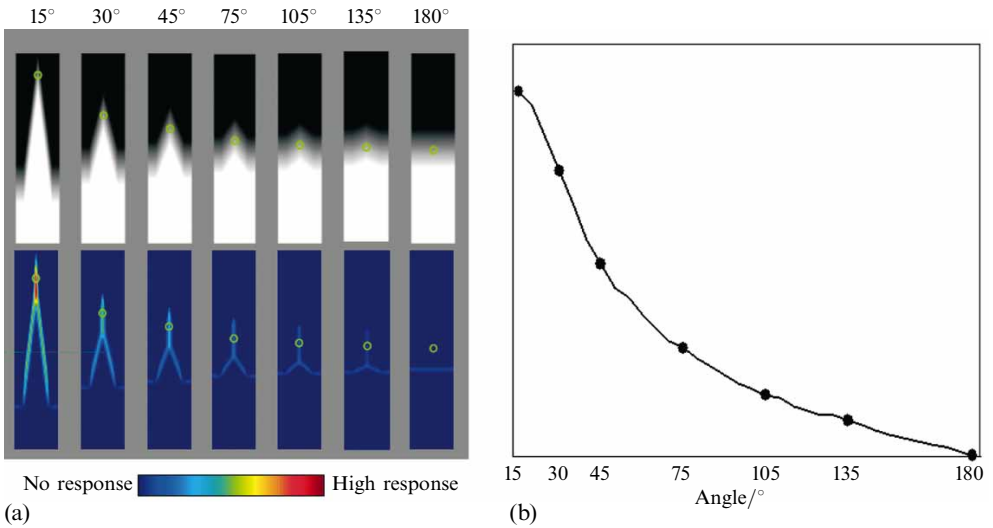
PSE for the angle tested (figure 4b). We found that the perceived salience of the corner varied linearly with the angle of the corner (independently of the interactions between angle polarity and gradient direction). Sharp angles generated stronger illusory salience than shallow angles (CASV). The results shown here for the average of all subjects ( $n = 12$ ) were consistent with individual averages (data not shown).

Figure 4c shows the same results, but conditions (1) and (2) (triangle symbols) are plotted separately from conditions (3) and (4) (square symbols). PSEs for conditions (1) and (2) were higher than the PSE for the control, whereas PSEs for conditions (3) and (4) were lower than the PSE for the control (CABR). The relationship between the angle of the corner and its perceived brightness/darkness was approximately linear in all conditions (figure 4d).

### 3.3 Center – surround simulations

In 1981, Hurvich proposed that Vasarely's nested-squares illusion could be accounted for by center–surround receptive fields (Hurvich 1981). Center–surround receptive fields and lateral inhibitory processes have also been proposed to explain other classical brightness illusions, such as the Hermann grid (Hermann 1870; Baumgartner 1960, 1961; Spillmann 1971), Mach bands (Mach 1865; von Békésy 1960; Ratliff 1965), and Chevreul's staircase (Chevreul 1839). Hurvich's basic idea was that the contrast between the center and the surround regions of the receptive field would be stronger along the corner gradients than along the edge gradients in a nested-square pattern, resulting in increased perceptual salience at the corners. We wondered whether the psychophysical results described here could be accounted for by an extension of Hurvich's center–surround model of Vasarely's nested-squares illusion, now applied more generally to corner gradients of all angles. To test this possibility, we modeled center–surround receptive fields as DOG filters (Rodieck 1965; Enroth-Cugell and Robson 1966); see section 2 for details. We chose the size of the DOG filter to match a range of physiological center–surround receptive fields in the primate LGN (Derrington and Lennie 1984; Irvin et al 1993; Tadmor and Tolhurst 2000; Levitt et al 2001) at the eccentricity used during the psychophysical experiments ( $3^\circ$ ). Both center and surround had the same weight towards the filter's output. Figure 5 shows the results of convolving a DOG filter ( $r_c$ : 0.18 deg;  $r_s$ : 0.36 deg) with the stimuli presented during the psychophysical experiments.

We found that the predicted strength of the effect varied in correlation to the angle of the corner, with sharp angles producing stronger outputs. However, the relationship between the angle of the corner and the strength of the response was not linear, whereas the psychophysical relationship was linear (figures 4b and 4d). Thus the qualitative aspects of the CASV effect (ie the correlation between the effect and the angle of the corner) are predicted by a simple DOG model, but the linear relationship between the corner angle and the strength of the effect that we found psychophysically is not accounted for. Other DOG filter parameters (such as different filter sizes, or different weights between the center and surround) tended to predict the same basic nonlinear result, with some variation in the shape of the curve (data not shown). Two main possibilities may account for this discrepancy: (a) the psychophysical effects are not fully accounted for by center–surround neurons, or (b) the psychophysical effects are fully explained by center–surround neurons, but simple DOG linear filters are not accurate models of center–surround receptive fields. These possibilities are, moreover, not mutually exclusive. We are currently conducting physiological recordings from LGN neurons in the awake primate while presenting equivalent stimuli, in order to distinguish between these two alternatives.



**Figure 5.** Computational simulations with a DOG filter. The filter parameters were chosen to match physiological center-surround receptive fields at the eccentricity used in the psychophysical experiments ( $3^\circ$ ). (a) Top: examples of corner-gradient stimuli analyzed in the simulations (dark-to-bright gradients, upwards angles). These stimuli were equivalent to the comparators [condition (1)] in the psychophysical experiment. The green circles mark the point of 50% luminance. (a) Bottom: convolving the DOG filter with the stimuli at the top simulates the output of an array of center-surround neurons. The green circles indicate the responses of the model at the point of 50% luminance on the actual gradient. (b) Predicted responses, at the point of 50% luminance on the corner gradient, for angles between  $15^\circ$  and  $180^\circ$  (in  $5^\circ$  steps). The data points indicate the angles used in the psychophysical experiment.

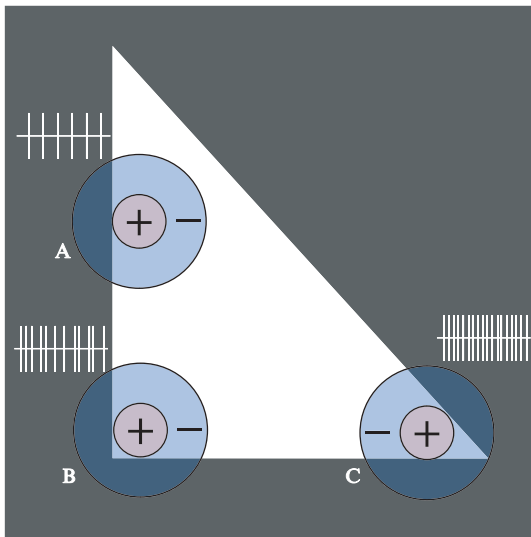


**Figure 6.** Generalized model of corner processing. Three on-center receptive fields are respectively placed over one edge and two corners of a white triangle. The center of the receptive field over the edge (position A) is well stimulated by light, but most of the surround also falls in the light region, so the response of the neuron is partially inhibited. The center of the receptive field over the  $90^\circ$  corner (position B) is also stimulated by light and most of the surround falls in the dark area. This is a more optimal stimulus than in (A) and leads to a stronger neural response. The receptive field over the  $45^\circ$  corner (position C) receives even more optimal contrast between center and surround, leading to an even stronger response. The spiking responses depicted in the cartoon are hypothetical.



---

## 4 Discussion

The information transmitted by our visual system is constrained by physical limitations, such as the relatively small number of axons available in the optic nerve. To some extent, our visual system overcomes these limitations by extracting, emphasizing, and processing non-redundant visual features. In 1961, Barlow proposed that the brain recodes visual data “so that their redundancy is reduced but comparatively little information is lost”. This idea is known as the “redundancy-reducing hypothesis” (Barlow 1961, 1989). The redundancy-reducing hypothesis has been invoked as an explanation for why neurons at the early levels of the visual system are suited to perform ‘edge-detection’, or ‘contour-extraction’. However, redundancy reduction is not necessarily constrained to edges, but rather should theoretically apply to any feature in the visual scene (Rao et al 2002). Just as edges are a less redundant feature than diffuse light, Attneave proposed in the 1950s that “points of maximum curvature” (ie discontinuities in edges, such as curves, angles, and corners—any point at which straight lines are deflected) are even less redundant than edges themselves, and thus contain more information (Attneave 1954). If points of high curvature are less redundant than points of low curvature, then sharp corners should also be less redundant than shallow corners. This leads to our prediction that, according to the redundancy-reducing hypothesis, sharp corners should appear to be perceptually more salient than shallow corners, which we show here psychophysically.

### 4.1 *Neural correlates of corner perception in the early visual system*

Our perception of the visual world is constructed in stages by neurons in sequential visual areas of the brain (Hubel and Wiesel 1962; Desimone et al 1980; Shipp and Zeki 1985; Felleman and Van Essen 1991). While feedback certainly plays a role in the visual system (Hupé et al 1998; Martinez-Conde et al 1999; Murphy et al 1999), the overall tendency of the visual system is comparable to a hierarchy, in which neurons in sequential levels extract more and more complicated features from the visual scene in a step-by-step manner. Several studies have emphasized the role of curves and corners in shape analysis and visual search (Watt 1988; Wolfe et al 1992; Kristjansson and Tse 2001; Tse 2002). However, theories of shape perception have typically been built on the premise that the primary step is the detection of visual edges. The predisposition of the visual system for edges versus diffuse light has been shown in physiological and perceptual studies (Mach 1865; Hubel and Wiesel 1959; Ratliff and Hartline 1959; Livingstone et al 1996; Macknik and Haglund 1999; Macknik et al 2000). Theoretical and physiological models of vision have thus assigned the function of ‘edge detector’ to early visual neurons (Marr and Hildreth 1980), whereas corner detection has been considered a cortical process, subsequent to edge detection (Hubel and Wiesel 1965; Dobbins et al 1987; Versavel et al 1990; Sillito et al 1995; Shevelev et al 1998; Das and Gilbert 1999; Pack et al 2003). In agreement with this idea, several studies of shape processing have invoked curves and corners as intermediate shape primitives (Milner 1974; Biederman 1987; Ullman 1989; Poggio and Edelman 1990; Dickinson et al 1992; Pasupathy and Connor 1999).

Vasarely's nested-squares illusion and the related effects described here show that corners are perceptually more salient than straight edges, and, moreover, that sharp corners are more salient than shallow corners. Hurvich's center-surround model of Vasarely's nested squares predicts that the 90° corner-gradient effects in the artwork arise from subcortical center-surround receptive fields. Moreover, Marr's primal sketch has also been shown to highlight corners (Watt 1988). Here we propose that Hurvich's hypothesis may be extended into a general model of corner processing in the early visual system, as the geometry of retinogeniculate center-surround receptive fields makes them, in general, better corner detectors than edge detectors (figure 6). It is possible

that center-surround receptive fields may have evolved to make use of the reduced redundancy of sharp corners versus shallow corners and edges. Because subsequent receptive field types (for instance, elongated simple-cell and complex-cell receptive fields in area V1) integrate visual information from subcortical levels (Hubel and Wiesel 1962; Tanaka 1983; Ferster 1986; Reid and Alonso 1995; Ferster et al 1996; Alonso and Martinez 1998; Martinez and Alonso 2001), cortical receptive fields should also be better tuned to corner detection than to edge detection. Thus, while it seems likely that curves and corners play an important role during high-level object recognition and shape processing, corner and curve detection may first take place within the lowest levels of the visual system, rather than within mid-level circuits.

The computational results shown here (figure 5) predict the general trend of the perceptual observations (ie that the strength of the percept varies inversely with the angle of the corner). However, they fail to predict the exact shape of the quantitative psychophysical results. Previous computational studies have proposed that linear receptive fields cannot process curvature features (Zetzsche and Barth 1990; Barth and Zetzsche 1998; Mota and Barth 2000) or some simultaneous contrast illusions (Morrone et al 1986). Thus, it is possible that center-surround receptive fields do not fully account for these illusions, and that further cortical processing takes place after the retinal/LGN levels. However, it is also possible that the simple DOG filters used here (despite the fact that we varied many of their parameters) are too rudimentary to completely simulate subcortical function. We are therefore currently carrying out electrophysiological recordings in the LGN and area V1 of the awake primate, using stimuli equivalent to the ones presented here, to distinguish between these two possibilities.

**Acknowledgments.** We thank Joan López-Moliner and Naoshige Uchida for advice on data analysis, Shannon Bentz for technical assistance, and Thomas Dyar for programming. These experiments were funded through a startup award from the Barrow Neurological Foundation to SM-C. XGT is a fellow of the Caixa Galicia Foundation.

## References

- Adelson E H, 1999 "Lightness perception and lightness illusions", in *The Cognitive Neurosciences* Ed. M S Gazzaniga (Cambridge, MA: MIT Press) pp 339–351
- Alonso J M, Martinez L M, 1998 "Functional connectivity between simple cells and complex cells in cat striate cortex" *Nature Neuroscience* **1** 395–403
- Attneave F, 1954 "Some informational aspects of visual perception" *Psychological Review* **61** 183–193
- Barlow H B, 1961 "Possible principles underlying the transformation of sensory messages", in *Sensory Communication* Ed. W A Rosenblith (Cambridge, MA: MIT Press) pp 217–234
- Barlow H B, 1989 "Unsupervised learning" *Neural Computation* **1** 295–311
- Barth E, Zetzsche C, 1998 "Endstopped operators based on iterated nonlinear center-surround inhibition", in *Human Vision and Electronic Imaging III* Eds B E Rogowitz, N P Pappas (SPIE **3299**) pp 67–78
- Baumgartner G, 1960 "Indirekte Größenbestimmung der rezeptiven Felder der Retina beim Menschen mittels der Hermannschen Gittertäuschung" *Pflügers Archiv für die gesamte Physiologie* **272** 21–22 (abstract)
- Baumgartner G, 1961 "Die Reaktionen der Neurone des zentralen visuellen Systems der Katze im simultanen Helligkeitskontrast", in *Neurophysiologie und Psychophysik des visuellen Systems* Eds R Jung, H H Kornhuber (Berlin, Göttingen, Heidelberg: Springer) pp 296–313
- Békésy G von, 1960 "Neural inhibitory units of the eye and the skin. Quantitative description of contrast phenomena" *Journal of the Optical Society of America* **50** 1060–1070
- Békésy G von, 1968 "Brightness distribution across the Mach bands measured with flicker photometry, and the linearity of sensory nervous interaction" *Journal of the Optical Society of America* **58** 1–8
- Biederman I, 1987 "Recognition-by-components: a theory of human image understanding" *Psychological Review* **94** 115–147
- Chevreul M E, 1839 *De la loi du contraste simultané des couleurs, et de l'assortiment des objets colorés* (Paris: Pitois-Levreault), English translation: *The Principles of Harmony and Contrast of Colors and Their Applications to the Arts* Ed. F Birren (1987, West Chester, PA: Schiffer Publishing)

- Das A, Gilbert C D, 1999 "Topography of contextual modulations mediated by short-range interactions in primary visual cortex" *Nature* **399** 655–661
- Derrington A M, Lennie P, 1984 "Spatial and temporal contrast sensitivities of neurones in lateral geniculate nucleus of macaque" *Journal of Physiology* **357** 219–240
- Desimone R, Fleming J, Gross C G, 1980 "Prestriate afferents to inferior temporal cortex: an HRP study" *Brain Research* **184** 41–55
- Dickinson S J, Pentland A P, Rosenfeld A, 1992 "From volumes to views: an approach to 3-D object recognition" *CVGP: Image Understanding* **55** 130–154
- Dobbins A, Zucker S W, Cynader M S, 1987 "Endstopped neurons in the visual cortex as a substrate for calculating curvature" *Nature* **329** 438–441
- Enroth-Cugell C, Robson J G, 1966 "The contrast sensitivity of retinal ganglion cells of the cat" *Journal of Physiology* **187** 517–552
- Felleman D J, Van Essen D C, 1991 "Distributed hierarchical processing in the primate cerebral cortex" *Cerebral Cortex* **1** 1–47
- Ferster D, 1986 "Orientation selectivity of synaptic potentials in neurons of cat primary visual cortex" *Journal of Neuroscience* **6** 1284–1301
- Ferster D, Chung S, Wheat H, 1996 "Orientation selectivity of thalamic input to simple cells of cat visual cortex" *Nature* **380** 249–252
- Hermann L, 1870 "Eine Erscheinung des simultanen Contrastes" *Pflügers Archiv für die gesamte Physiologie* **3** 13–15
- Hubel D H, Wiesel T N, 1959 "Receptive fields of single neurones in the cat's striate cortex" *Journal of Physiology* **148** 574–591
- Hubel D H, Wiesel T N, 1962 "Receptive fields, binocular interaction and functional architecture in the cat's visual cortex" *Journal of Physiology* **160** 106–154
- Hubel D H, Wiesel T N, 1965 "Receptive fields and functional architecture in two non-striate visual areas (18 and 19) of the cat" *Journal of Neurophysiology* **28** 229–289
- Hupé J M, James A C, Payne B R, Lomber S G, Girard P, Bullier J, 1998 "Cortical feedback improves discrimination between figure and background by V1, V2 and V3 neurons" *Nature* **394** 784–787
- Hurvich L M, 1981 *Color Vision* (Sunderland: Sinauer Associates)
- Irvin G E, Casagrande V A, Norton T T, 1993 "Center/surround relationships of magnocellular, parvocellular, and koniocellular relay cells in primate lateral geniculate nucleus" *Visual Neuroscience* **10** 363–373
- Kaiser P K, 1996 "The joy of visual perception: A web book", <http://www.yorku.ca/eye/thejoy.htm>
- Kristjansson A, Tse P U, 2001 "Curvature discontinuities are cues for rapid shape analysis" *Perception & Psychophysics* **63** 390–403
- Levitt J B, Schumer R A, Sherman S M, Spear P D, Movshon J A, 2001 "Visual response properties of neurons in the LGN of normally reared and visually deprived Macaque monkeys" *Journal of Neurophysiology* **85** 2111–2129
- Livingstone M S, Freeman D C, Hubel D H, 1996 "Visual responses in V1 of freely viewing monkeys" *Cold Spring Harbor Symposia on Quantitative Biology* **LXI** 27–37
- McArthur J A, Moulden B, 1999 "A two-dimensional model of brightness perception based on spatial filtering consistent with retinal processing" *Vision Research* **39** 1199–1219
- Mach E, 1865 "Über die Wirkung der räumlichen Verteilung des Lichtreizes auf der Netzhaut" *Sitzungsberichte der mathematisch-naturwissenschaftlichen Classe der kaiserlichen Akademie der Wissenschaften* **52** 303–322 [Translated by Ratliff (1965)]
- Macknik S L, Haglund M M, 1999 "Optical images of visible and invisible percepts in the primary visual cortex of primates" *Proceedings of the National Academy of Sciences of the USA* **96** 15208–15210
- Macknik S L, Martinez-Conde S, Haglund M M, 2000 "The role of spatiotemporal edges in visibility and visual masking" *Proceedings of the National Academy of Sciences of the USA* **97** 7556–7560
- Marr D, Hildreth E, 1980 "Theory of edge detection" *Proceedings of the Royal Society of London, Series B* **207** 187–217
- Martinez L M, Alonso J M, 2001 "Construction of complex receptive fields in cat primary visual cortex" *Neuron* **32** 515–525
- Martinez-Conde S, Cudeiro J, Grieve K L, Rodriguez R, Rivadulla C, Acuna C, 1999 "Effects of feedback projections from area 18 layers 2/3 to area 17 layers 2/3 in the cat visual cortex" *Journal of Neurophysiology* **82** 2667–2675

- Martinez-Conde S, Macknik S L, 2001 "Junctions are the most salient visual features in the early visual system", in *Society for Neuroscience 31st Annual Meeting* (San Diego, CA: Society for Neuroscience)
- Milner P M, 1974 "A model for visual shape recognition" *Psychological Review* **81** 521–535
- Morgan M J, 1996 "Visual illusions", in *Unsolved Mysteries Of The Mind: Tutorial Essays in Cognition* Ed. V Bruce (Hove: Lawrence Erlbaum Associates) pp 29–58
- Morrone M C, Ross J, Burr D C, 1986 "Mach bands are phase dependent" *Nature* **324** 250–253
- Mota C, Barth E, 2000 "On the uniqueness of curvature features" *Proceedings in Artificial Intelligence* **9** 175–178
- Murphy P C, Duckett S G, Sillito A M, 1999 "Feedback connections to the lateral geniculate nucleus and cortical response properties" *Science* **286** 1552–1554
- Pack C C, Livingstone M S, Duffy K R, Born R T, 2003 "End-stopping and the aperture problem: two-dimensional motion signals in macaque V1" *Neuron* **39** 671–680
- Pasupathy A, Connor C E, 1999 "Responses to contour features in macaque area V4" *Journal of Neurophysiology* **82** 2490–2502
- Poggio T, Edelman S, 1990 "A network that learns to recognize three-dimensional objects" *Nature* **343** 263–266
- Rao R P N, Olshausen B A, Lewicki M S, 2002 *Probabilistic Models of the Brain: Perception and Neural Function* (Cambridge, MA: MIT Press)
- Ratliff F, 1965 *Mach Bands: Quantitative Studies on Neural Networks in the Retina* (San Francisco, CA: Holden-Day)
- Ratliff F, Hartline H K, 1959 "The responses of Limulus optic nerve fibers to patterns of illumination on the receptor mosaic" *Journal of General Physiology* **42** 1241–1255
- Reid R C, Alonso J M, 1995 "Specificity of monosynaptic connections from thalamus to visual cortex" *Nature* **378** 281–284
- Rodieck R W, 1965 "Quantitative analysis of cat retinal ganglion cell response to visual stimuli" *Vision Research* **5** 583–601
- Shevelev I A, Lazareva N A, Sharaev G A, Novikova R V, Tikhomirov A S, 1998 "Selective and invariant sensitivity to crosses and corners in cat striate neurons" *Neuroscience* **84** 713–721
- Shipp S, Zeki S, 1985 "Segregation of pathways leading from area V2 to areas V4 and V5 of macaque monkey visual cortex" *Nature* **315** 322–325
- Sillito A M, Grieve K L, Jones H E, Cudeiro J, Davis J, 1995 "Visual cortical mechanisms detecting focal orientation discontinuities" *Nature* **378** 492–496
- Spillmann L, 1971 "Foveal perceptive fields in the human visual system measured with simultaneous contrast in grids and bars" *Pflügers Archiv für die gesamte Physiologie* **326** 281–299
- Tadmor Y, Tolhurst D J, 2000 "Calculating the contrasts that retinal ganglion cells and LGN neurons encounter in natural scenes" *Vision Research* **40** 3145–3157
- Tanaka K, 1983 "Cross-correlation analysis of geniculostriate neuronal relationships in cats" *Journal of Neurophysiology* **49** 1303–1318
- Tse P U, 2002 "A contour propagation approach to surface filling-in and volume formation" *Psychological Review* **109** 91–115
- Ullman S, 1989 "Aligning pictorial descriptions: an approach to object recognition" *Cognition* **32** 193–254
- Vasarely V, 1970 *Vasarely II* (Neuchâtel: Éditions du Griffon)
- Vasarely V, 1982 *Gea* (Paris: Éditions Hervas)
- Versavel M, Orban G A, Lagae L, 1990 "Responses of visual cortical neurons to curved stimuli and chevrons" *Vision Research* **30** 235–248
- Watt R J, 1988 *Visual Processing: Computational, Psychophysical and Cognitive Research* (Hove, Sussex: Lawrence Erlbaum Associates)
- Wichmann F A, Hill N J, 2001 "The psychometric function: I. Fitting, sampling, and goodness of fit" *Perception & Psychophysics* **63** 1293–1313
- Wolfe J M, Yee A, Friedman-Hill S R, 1992 "Curvature is a basic feature for visual search tasks" *Perception* **21** 465–480
- Zetsche C, Barth E, 1990 "Fundamental limits of linear filters in the visual processing of two-dimensional signals" *Vision Research* **30** 1111–1117

ISSN 0301-0066 (print)

ISSN 1468-4233 (electronic)

# PERCEPTION

VOLUME 34 2005

[www.perceptionweb.com](http://www.perceptionweb.com)

**Conditions of use.** This article may be downloaded from the Perception website for personal research by members of subscribing organisations. Authors are entitled to distribute their own article (in printed form or by e-mail) to up to 50 people. This PDF may not be placed on any website (or other online distribution system) without permission of the publisher.